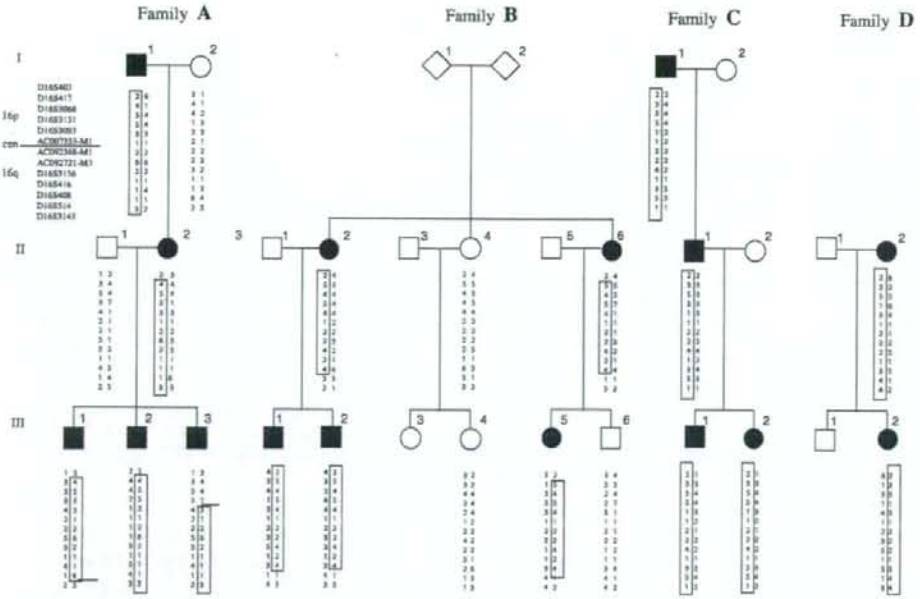

Fig. 2 Haplotype analysis of the four new PKC families (Families A–D). The *numbers in boxes* represent putative disease haplotypes. The *heavy short lines* indicate recombination sites

nih.gov/SNP/). Seven of the alterations in six genes were nonsynonymous substitutions resulting in amino-acid substitutions (Table 2). Five of such nonsynonymous substitutions in four genes were observed both in some patients and among 100 normal control individuals. The remaining two, i.e., 6186C>A in exon 3 of *SCNN1G* (the gene for sodium channel, nonvoltage-gated 1, gamma) and 45842A>G in exon 29 of *ITGAL* (the integrin alpha L precursor gene), observed in Families C and F, respectively, were not observed among more than 400 normal controls. The real-time quantitative PCR analysis did not detect a duplication or a deletion within the two genes. Of the 35 intronic base changes we identified in the seven patients, none were located at the acceptor or donor splice sites (Fig. 3).

G-banding chromosome analysis at the 400-band level and C-banding analysis revealed that all five patients from Families B–D, F, and G had a normal-sized heterochromatin block on chromosome 16 without an inversion (data not shown).

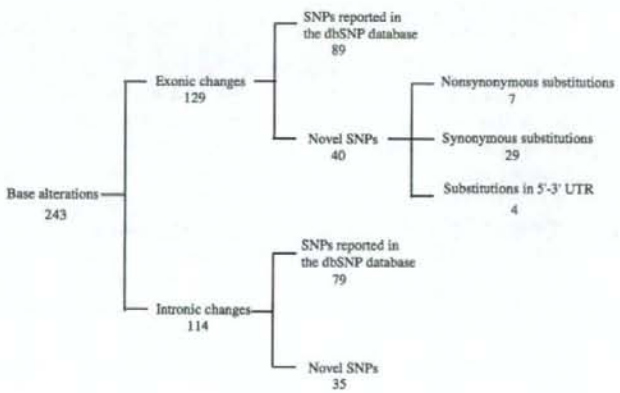

Fig. 3 Classification of 243 base alterations in 157 candidate genes. Information of the newly found single nucleotide polymorphisms (SNPs) is shown in Table 2. None of the novel intronic SNPs are located at any of the acceptor or donor splice sites

Table 2 List of genes for mutation analysis in the PKC patients, and novel SNPs identified, their positions, nucleotide changes, and amino acid changes

Gene	E/I	SNP definition	AA	Gene	E/I	SNP definition	AA	Gene	E/I	SNP definition	AA
HS3ST2*				ASPHD1	E1	515insTGG		ITGAX*			
SCNN1G*	E3	6185G>T	Y241Y	KCTD13*	I2	INV2-74A>T		ITGAD*	5′U	5′U-13G>C*	
	E3	6186C>A	P242T	LOC124446					E2	943C>T	G33G
SCNN1B*				TAOK2*					I7	INV7+38C>T	
UBPH*				HIRIP3*					E8	14188A>G	R246R
NDUFAB1*				CCDC95					E8	14253A>G	Y268C
PRKCB1*	E1	79C>A	R27R	DOC2A*					I9	INV10-43G>A	
	I15	INV15+85G>T		FAM57B	I2	INV2+66G>T			E16	19819A>G	S644G
CACNG3*				ALDOA*					I17	INV17+139G>A	
TNRC6A*	E1	5′U-12079T>A		PPP4C*	E1	5′U-355-347del(CGG)3			I19	INV19+71C>T	
	E21	33511C>T	H1551H	TBX6*					I27	INV27+87G>A	
SLC5A11*	I1	5′U-12193T>C		YPEL3*				ARMC5*			
	I2	INV2+6C>G		GDPD3				TGFB1I1*	E5	753C>T	P119S
	I5	INV5-30G>A		MAPK3*				SLC5A2*			
	I5	INV5+65T>C		CORO1A*				C16orf58*	I5	INV5+53G>A	
LCMT1*				SULT1A3*				ERAF*	3′U	3′U+570T>C*	
IL4R*	I3	INV3+72T>A		CD2BBP2*	I1	INV1+493C>T		MGC3020*			
	E11	22448T>C	L433L	TBC1D10B*				ZNF720*			
IL21R*	I4	INV4+51C>T		MYLPF	I5	INV5+27G>A		ZNF267			
GTF3C1*				SEPT1*				TP53TG3*	E3	1232insG	
KIAA0556*	I16	INV16+4T>C		ZNF553	E2	2434G>A	T326T	FLJ43855			
	E18	204044A>G	Q1198Q	ZNF771				POL3S			
GSGIL*				XTP3TPA*				FLJ46121			
XPO6*	I9	INV9+31insT		SEPHS2*				FLJ43980	E1	5′U-15C>G	
	I15	INV15+23G>C		ITGAL*	E1	5′U-86C>T		SHCBP1*	E5	12986C>T	N204N
	E16	69120T>C	N740N		E29	45842A>G	K1063R	VPS35*			
SBK-1				ZNE768				ORC6L	E6	6328A>G	V193V
LOC440350				ZNF747				MLCK*			
LOC440348				ZNF764				LOC388272*			
CLN3*	I12	INV12+36C>T		ZNF688				GPT2*			
	E15	14138A>G	H404R	ZNF785				DNAJA2*			
APOB48R*				ZNF689				NETO2*	I3	INV3-34G>A	
IL27*	I5	INV5-12C>T		PRR14				ITFG1 *			
NUPR1*				FBS1*				PHKB*	I28	INV28+37C>T	
CCDC101*				SRCAP*				ABCC12*			
SULT1A2*				PHKG2*				ABCC11*			
SULT1A1*				LOC90835				LONPL*			
EIF3S8*	E16	20499C>T	P725P	RNF40*				SIAH1			
ATXN2L*	I13	INV13+55G>A		BCL7C*				N4BP1*			
TUFM*				CTF1*				CBLN1*			
SH2B*				LOC283932				FLJ44674	E1	3′U+905C>G	
ATP2A1*				FBXL19*				C16orf78*	E1	45G>A	K15K
RABEP2*	I3	INV4-56C>T		TMEM142C					I3	INV3+27A>G	
CD19*	E4	1379G>T	P206P	SETD1A*				ZNF423 *			
SPIN1*	E7	6897C>T	S319S	HSD3B7*				C16orf69			
	I7	INV7+278Cdel		STX1B2*				HEATR3 *	I11	INV11-44A>G	
	3′U	3′U+9285C>A*		STX4A*	I8	INV8+55C>A		PAPD5*			
LAT	E7	1259G>A	A120A		I8	INV8+65C>T		ADCY7*	E22	24951T>C	Y875Y
BOLA2				ZNF668				BRD7*	I9	INV9-26insT	
GDYD1*				ZNF646*	I1	5′U-108T>G			E16	48481G>A	T570T
SPN*					E2	2722G>C	G907A	NKD1*			
QPRT*				VKORC1*	3′U	3′U+3730G>C*		SLIC1*			
C16orf54				BCKDK*				CARD15*			
KIF22*	I12	INV12+70A>G		MYST1*				CYLD*	E17	43909C>T	D805D
MAZ*				PRSS8*	E3	2163C>T	V46V	SALL1*			
PRRT2				PRSS36				FTS*			
MVP*	E10	11504C>T	D525D	FUS*				CAPNS2*			
C16orf53				TRIM72				SLC6A2*			
CDIPT*				PYCARD*				GNAO1*			
PSK-1*				PYDC1*				CNGB1*	E22	51134C>T	N725N
				ITGAM*	I2	INV2+11T>C					

A total of 75 SNPs not reported in the dbSNP database were found in this study

Four SNPs found in 5′-UTR or 3′-UTR happened to be included in the sequenced regions

*Analyzed in seven representative patients: E/I=exon or intron; AA=inferred amino acid change from nonsynonymous SNP; U=UTR

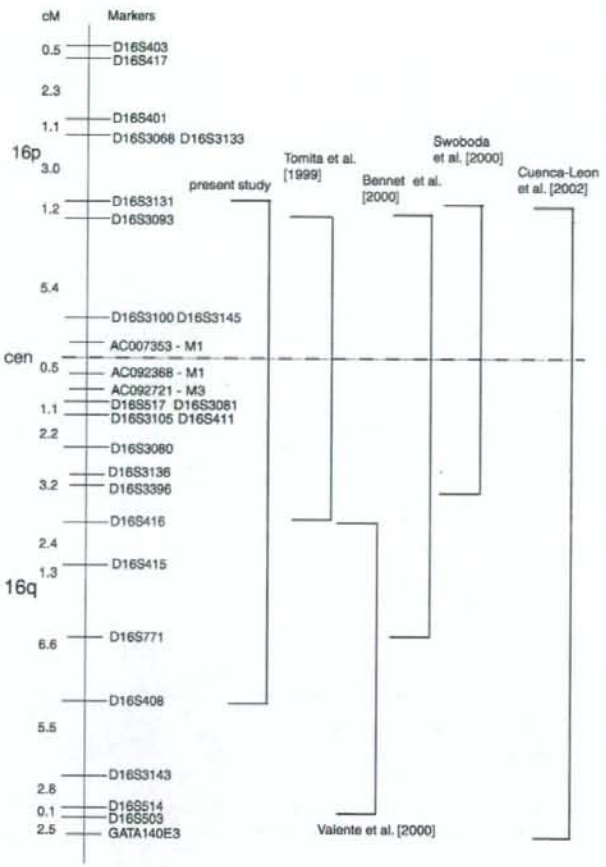

Fig. 4 The PKC-critical region (PKCCR) summarized by five mapping studies (Tomita et al. 1999; Bennett et al. 2000; Swoboda et al. 2000; Cuenca-Leon et al. 2002, present study), as well as a seemingly second PKC locus (EKD2) by Valente et al. (2000). The location of markers and intermarker distances are from the Généthon map (Dib et al. 1996)

Table 3 List of exons that have not been sequenced in the mutation analysis

Gene	Exon
COX6A2	Exon 2, Exon 3
MAZ	Exon 1, Exon 2, Exon 3
VPS35	Exon 9, Exon 10, Exon 11
SULT1A1	Exon 7
SALL1	Exon 2
MGC2474	Exon 2
FLJ43855	Exon 5, Exon 7, Exon 9

Discussion

The PKCCR was assigned to a segment between *D16S3093* and *D16S416* in eight Japanese families (Tomita et al. 1999). It was also mapped between *D16S3100* and *D16S771* in an Afro-Caribbean family (Bennett et al. 2000), between *D16S3131* and *D16S3396* in 11 families of diverse ethnicity (Swoboda et al. 2000), between *D16S3145* and *GATA140E03* in a Spanish family (Cuenca-Leon et al. 2002), and a 24-cM segment between *D16S3131* and *D16S408* in the present study (Fig. 4). Thus, the shortest region of overlap (SRO) did not become narrower than a 12.4-cM segment detected by Tomita et al. (1999). Valente et al. (2000) assigned a form of PKC (a second PKC locus, EKD2), in an Indian family, to a segment between *D16S416* and *D16S503*, the region distinct from those mapped by Tomita et al. (1999) and by Swoboda et al. (2000). Furthermore, two other clinical entities, ICCA and BFIC2, were assigned to a region encompassing the centromere of chromosome 16 (Lee et al. 1998; Hattori et al. 2000; Swoboda et al. 2000; Caraballo et al. 2001; Weber et al. 2004). Since all of these loci were confined to a relatively small region, it is likely that all of these paroxysmal movement dis-

orders actually belong to one disorder and are allelic, as suggested previously (Tomita et al. 1999).

We searched for mutations in almost all protein-coding genes mapped at the PKCCR. In addition, we also analyzed four ion-channel-related genes (*CACNG3*, *SCNN1B*, *SCNN1G*, and *CNGB1*), albeit located outside the PKCCR, since many episodic neurologic disorders, such as muscle diseases, epilepsy, and movement disorders, are known as ion-channel abnormalities (Bhatia et al. 2000). However, 14 coding exons in seven genes (Table 3) were not analyzed because of difficulties in PCR-amplification.

In the present study on a total of 157 genes, we failed to identify any causative mutations that can explain PKC in all of the seven families examined. However, two nonsynonymous substitutions, 6186C>A in exon 3 of *SCNN1G* and 45842A>G in exon 29 of *ITGAL*, which were co-segregated with PKC in Families C and F, respectively, which were not found in normal control individuals, might be implicated in PKC. In other words, they were not able to be totally ruled out from the candidacy for PKC. It thus remains to be investigated whether another mutation in either gene is found in other PKC families.

Although the mapping of PKC was successful in at least nine studies, causative mutations have been uncovered. This may imply that PKC is caused by aberrations other than exonic mutations, such as a deletion or insertion, in the promoter regions, including the 5′-UTR or 3′-UTR. However, there is still a possibility for usual exonic mutations in a novel gene not annotated in public databases. As PKC itself is, generally, a viable disorder with which patients may show high reproductive fitness, such a mutated allele may be transmitted through many generations. A chromosomal rearrangement is another possibility. The pericentromeric region of chromosome 16 has a large heterochromatin (C-band) block that contains several duplicated regions, through which, frequent chromosomal rearrangements occur (Loftus et al. 1999). It remains also to be seen whether PKC patients within a family share such a variant.

Acknowledgments We are indebted to the family members for their participation in this research. We especially thank Ms. Y. Noguchi and A. Goto for their technical assistance. N.N. was supported in part by a Grant-in-Aid for Scientific Research (Category S, grant no. 13854024; Priority Areas for Applied Genomics, grant no. 17019055) from the Ministry of Education, Culture, Sports, Science and Technology (MEXT) of Japan, and by Solution Oriented Research of Science and Technology (SORST) from the Japan Science and Technology Agency (JST). K.Y. was supported by a Grant-in-Aid for Scientific Research for Priority Areas (grant no. 17590288) from the MEXT of Japan.

References

Bennett LB, Roach ES, Bowcock AM (2000) A locus for paroxysmal kinesigenic dyskinesia maps to human chromosome 16. Neurology 54(1):125–130

Bhatia KP (1999) The paroxysmal dyskinesias. J Neurol 246(3):149–155

Bhatia KP, Griggs RC, Ptáček LJ (2000) Episodic movement disorders as channelopathies. Mov Disord 15(3):429–433

Caraballo R, Pavek S, Lemainque A, Gastaldi G, Echenne B, Motte J, Genton P, Cersósimo R, Humbertclaude V, Fejerman N, Monaco AP, Lathrop MG, Rochette J, Szepetowski P (2001) Linkage of benign familial infantile convulsions to chromosome 16p12-q12 suggests allelism to the infantile convulsions and choreoathetosis syndrome. Am J Hum Genet 68(3):788–794

Cuenca-Leon E, Cormand B, Thomson T, Macaya A (2002) Paroxysmal kinesigenic dyskinesia and generalized seizures: clinical and genetic analysis in a Spanish pedigree. Neuropediat 33(6):288–293

Dib C, Faure S, Fizames C, Samson D, Drouot N, Vignal A, Millasseau P, Marc S, Hazan J, Seboun E, Lathrop M, Gyapay G, Morissette J, Weissenbach J (1996) A comprehensive genetic map of the human genome based on 5246 microsatellites. Nature 380:152–154

Hattori H, Fujii T, Nigami H, Higuchi Y, Tsuji M, Hamada Y (2000) Co-segregation of benign infantile convulsions and paroxysmal kinesigenic choreoathetosis. Brain Develop 22(7):432–435

Kato N, Sadamatsu M, Kikuchi T, Niikawa N, Fukuyama Y (2006) Paroxysmal kinesigenic choreoathetosis: from first discovery in 1892 to genetic linkage with benign familial infantile convulsions. Epilepsy Res 70(Suppl 1):174–184

Lee W-L, Tay A, Ong H-T, Goh L-M, Monaco AP, Szepetowski P (1998) Association of infantile convulsions with paroxysmal dyskinesias (ICCA syndrome): confirmation of linkage to human chromosome 16p12-q12 in a Chinese family. Hum Genet 103(5):608–612

Loftus BJ, Kim UJ, Sneddon VP, Kalush F, Brandon R, Fuhrmann J, Mason T, Crosby ML, Barnstead M, Cronin L, Deslattes Mays A, Cao Y, Xu RX, Kang HL, Mitchell S, Eichler EE, Harris PC, Venter JC, Adams MD (1999) Genome duplications and other features in 12 Mb of DNA sequence from human chromosome 16p and 16q. Genomics 60(3):295–308

Nagamitsu S, Matsuishi T, Hashimoto K, Yamashita Y, Aihara M, Shimizu K, Mizuguchi M, Iwamoto H, Saitoh S, Hirano Y, Kato H, Fukuyama Y, Simada M (1999) Multicenter study of paroxysmal dyskinesias in Japan—clinical and pedigree analysis. Mov Disord 14(4):658–663

Sadamatsu M, Masui A, Sakai T, Kunugi H, Nanko S, Kato N (1999) Familial paroxysmal kinesigenic choreoathetosis: an electrophysiologic and genotypic analysis. Epilepsia 40(7):942–949

Swoboda KJ, Soong B, McKenna C, Brunt ER, Litt M, Bale JF Jr, Ashizawa T, Bennett LB, Bowcock AM, Roach ES, Gerson D, Matsuura T, Heydemann PT, Nespeca MP, Jankovic J, Leppert M, Ptáček LJ (2000) Paroxysmal kinesigenic dyskinesia and infantile convulsions: clinical and linkage studies. Neurology 55(2):224–230

Tomita H, Nagamitsu S, Wakui K, Fukushima Y, Yamada K, Sadamitsu M, Masui A, Konishi T, Matsuishi T, Aihara M, Shimizu K, Hashimoto K, Mineta M, Matsushima M, Tsujita T, Saito M, Tanaka H, Tsuji S, Takagi T, Nakamura Y, Nakano S, Kato N, Nakane Y, Niikawa N (1999) Paroxys-

mal kinesigenic choreoathetosis locus maps to chromosome 16p11.2-q12.1. Am J Hum Genet 65(6):1688–1697

Valente EM, Spacey SD, Wali GM, Bhatia KP, Dixon PH, Wood NW, Davis MB (2000) A second paroxysmal kinesigenic choreoathetosis locus (EKD2) mapping on 16q13-q22.1 indicates a family of genes which give rise to paroxysmal disorders on human chromosome 16. Brain 123(10):2040–2045

Weber YG, Berger A, Bebek N, Maier S, Karafyllakes S, Meyer N, Fukuyama Y, Halbach A, Hikel C, Kurlemann G, Neubauer B, Osawa M, Püst B, Rating D, Saito K, Stephani U, Tauer U, Lehmann-Horn F, Jurkat-Rott K, Lerche H (2004) Benign familial infantile convulsions: linkage to chromosome 16p12-q12 in 14 families. Epilepsia 45(6):601–609

American Journal of Medical Genetics Part A 146A:124–127 (2008)

Research Letter

A Girl With Down Syndrome and Partial Trisomy for 21pter-q22.13:

A Clue to Narrow the Down Syndrome Critical Region

Daisuke Sato,[1,2,3] Hiroki Kawara,[4] Osamu Shimokawa,[1,3,4] Naoki Harada,[3,4] Hidefumi Tonoki,[2,5,6] Nobuhiro Takahashi,[5] Yumi Imai,[6] Hiromi Kimura,[6] Naomichi Matsumoto,[3,7] Tadashi Ariga,[2] Norio Niikawa,[1,3] and Koh-ichiro Yoshiura[1,3]*

[1]Department of Human Genetics, Nagasaki University Graduate School of Biomedical Sciences, Nagasaki, Japan
[2]Department of Pediatrics, Hokkaido University Graduate School of Medicine, Sapporo, Japan
[3]Solution Oriented Research of Science and Technology (SORST), Japan Science and Technology Agency (JST), Kawaguchi, Japan
[4]Kyushu Medical Science, Nagasaki, Japan
[5]Department of Pediatrics, Caress Alliance Medical Corporation, Tenshi Hospital, Sapporo, Japan
[6]Section of Clinical Genetics, Caress Alliance Medical Corporation, Sapporo, Japan
[7]Department of Human Genetics, Yokohama City Graduate School of Medicine, Yokohama, Japan

Received 28 January 2007; Accepted 26 May 2007

How to cite this article: Sato D, Kawara H, Shimokawa O, Harada N, Tonoki H, Takahashi N, Imai Y, Kimura H, Matsumoto N, Ariga T, Niikawa N, Yoshiura K. 2008. A girl with Down syndrome and partial trisomy for 21pter-q22.13: A clue to narrow the Down syndrome critical region. Am J Med Genet Part A 146A:124–127.

To the Editor:

Down syndrome (DS) is the most common multiple congenital anomaly syndrome with mental retardation. The majority of patients with DS have full trisomy for chromosome 21, but rare patients have partial trisomy 21, indicating the presence of a DS critical region (DSCR) that contains genes contributing to cognitive defects and/or other DS features [Antonarakis et al., 2004]. The DSCR has been narrowed down to a region within 21q22, about 5.4 Mb in length [Delabar et al., 1993; Arron et al., 2006]. Here, we describe a girl with DS and a novel karyotype that may narrow the DSCR down to 2.3 Mb.

The Japanese girl was born with a birthweight of 2,964 g (−0.3 SD), length of 46.8 cm (−1.1 SD) and OFC of 33.0 cm (mean) after 38 weeks gestation to a 22-year-old mother and a 30-year-old father. Diagnosis of DS was made soon after birth. Echocardiogram showed PDA. Although further growth was within the normal range, developmental delay was severe. Physical examinations at age 16 months showed the following abnormalities: brachycephaly with flat occiput, epicanthus, strabismus, upslanting palpebral fissures, small nose with low nasal bridge, upturned nostrils, open mouth, protruding tongue, short neck (Fig. 1a,b), short and broad hands with short fifth fingers, congenital heart defect with heart murmur, joint hyperflexibility and muscular hypotonia. These are 13 of 25 signs and satisfied the criterion for a clinical diagnosis of DS according to the Jackson score [Jackson et al., 1976].

After written informed-consent was obtained from her parents, and the study protocol was approved by the Committee for Genetic Testing and Counseling, Tenshi Hospital, cytogenetic studies were performed. A 550-band-level G-banding analysis on her metaphase chromosomes from cultured peripheral blood lymphocytes revealed an isodicentric chromosome 21, 46,XX,idic(21)(q22) (Fig. 1c). Centromere-dot (Cd) banding revealed that one side of the centromere dots of the isochromosome was separated (data not shown). This finding indicated that one of the centromeres was inactivated; hence, the isochromosome was segregating stably [Maraschio et al., 1980]. Spectral karyotyping (SKY) analysis disclosed a more complex abnormality, that is, 46,XX,t(13;21),idic(21)(q22). This karyotype was confirmed by conventional fluorescence in situ hybridization (FISH) using whole-chromosome-painting probes for chromosomes 13 and 21 (Vysis, Downers Grove, IL; Fig. 1d). Additional FISH analysis

*Correspondence to: Koh-ichiro Yoshiura, M.D., Ph.D., Department of Human Genetics, Nagasaki University Graduate School of Biomedical Sciences, Sakamoto 1-12-4, Nagasaki 852-8523, Japan.
E-mail: kyoshi@net.nagasaki-u.ac.jp
DOI 10.1002/ajmg.a.31974

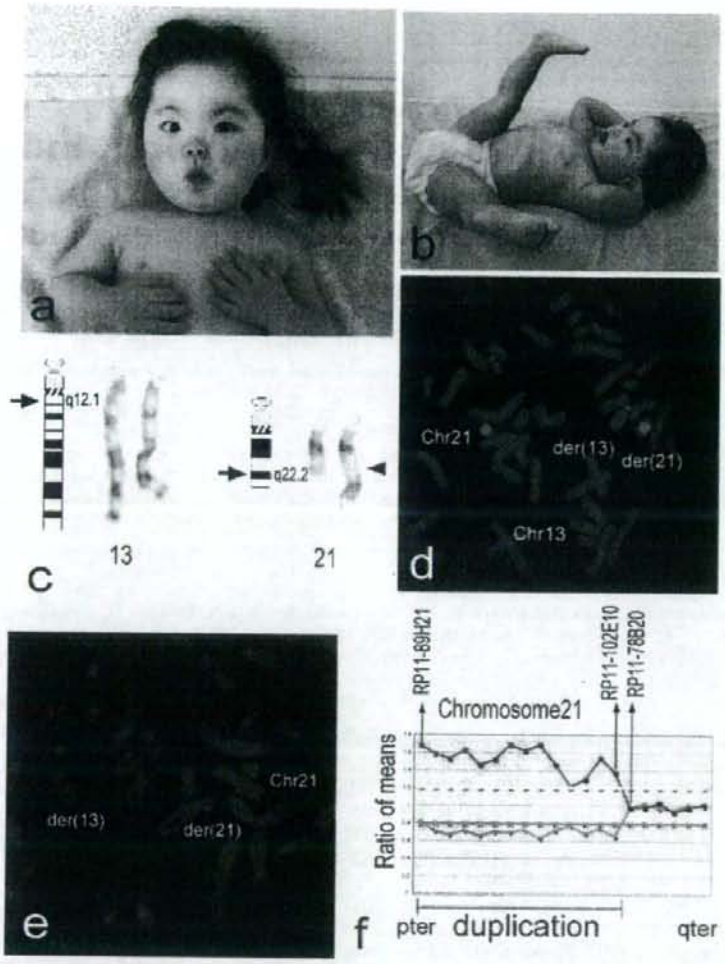

FIG. 1. **a**,**b**: The patient at age 16 months (a and b). **c**: G-banded partial karyotype of the patient. Arrows indicate the breakpoints of an inserted chromosome 13 and an isodicentric chromosome 21. **d**: FISH with chromosome-specific painting probes for chromosomes 13 (red) and 21 (green), showing an insertion of a chromosome 21-derived segment into a pericentromeric region of 13q. **e**: FISH using BAC-clone probes, RP11-1012D8 (green) and RP11-124E9 (red). Green signals appear on both der(13) and der(21) as well as normal chromosome 21, while red signals are seen on normal chromosome 21 and der(13), but not observed on der(21). **f**: Array CGH analysis demonstrates a duplication of a part of chromosome 21. The proximal and distal end clones within the duplication region were RP11-89H21 (21q11.2) and RP11-102E10 (21q22.13), respectively. The breakpoint of der (21) was suggested to be located between RP11-102E10 and RP11-78B20.

with a BAC clone (RP11-1012D8) located to 21q22.13 showed split signals both on der(13) and der(21) chromosomes as well as on normal chromosome 21. FISH using RP11-89H21 (21q11.2), RP11-166F15 (21q22.13), RP11-98O13 (21q22.13), RP11-183O20 (21q22.13), and RP11-95G19 (21q22.13) all gave signals only on both der(21) and normal chromosome 21, while signals appeared on both der(13) and normal chromosome 21 when using other BAC probes located more distantly, such as RP11-608F9 (21q22.13), RP11-749M19 (21q22.2), RP11-814F13 (21q22.3), RP11-124E9 (21q22.3), and RP11-135B17 (subtelomeric region). These analyses successfully identified the breakpoint of the isochromosome at band 21q22.13 (the UCSC genome browser, 2004 May version, http://genome.ucsc.edu/cgi-bin/hgGateway). As for the derivative chromosome 13, we could not define an insertion point precisely, because the insertion occurred closely to the centromeric region where no BAC probes were available. Within the insertion, a FISH signal for RP11-124E9 (SpectrumOrange) mapped at 21q22.3 was observed

proximally to that for RP11-1012D8 (Spectrum-Green) at 21q22.13 (Fig. 1e), demonstrating an inverted insertion on chromosome 13. All these findings indicated that the patient had partial trisomy for a 21pter-q22.13 segment, while her 21q22.13-qter region was disomic. The distal boundary of the trisomic segment lies at the region corresponding to the BAC clone, RP11-1012D8. As her parental karyotypes were normal in both Q-banding and SKY analyses, the patient's karyotype was interpreted as 46,XX,psu idic(21)(q22.13) ins(13;21)(q12.1;q22.13q22.3)dn (Fig. 2a). To know the presence of any other chromosomal aberrations, home-made whole-genome BAC-based microarray with 1.5 Mb resolution comparative genomic hybridization (array CGH) [Sato et al., 2007] was carried out using the patient's DNA. Consequently, the array CGH detected the same partial trisomy 21 (Fig. 1f), but no other deletion nor amplification in the genome.

The DSCR has always been somewhat controversial since many reports included were either premature for precise chromosome banding, include mosaic individuals, or resulted from familial translocations which may have involved undefined reciprocal deletions [Ronan et al., 2007]. Olson et al. [2004] reported that trisomy for the DSCR alone is insufficient and largely unnecessary to cause specific DS phenotypes in mice models. But, the suggestion may not be suitable for human because there are some differences between mouse and human gene content. Later, Olson et al. [2007] reported that trisomy for the DSCR is necessary for brain phenotypes of trisomic mice, thus the DSCR must have some association with the occurrence of DS. Furthermore, recent experiments using mouse models of DS suggested that a 1.5-fold increase in dosage of *DSCR1* and *DYRK1A* within the DSCR destabilizes a regulatory circuit in a cooperative way, contributing to the reduced NFATc activity and many of the characteristics of DS [Arron et al., 2006].

Interestingly, the trisomic segment of our patient partially overlaps the previously estimated DSCR at 21q22 and we have also confirmed that no known genes were disrupted at the breakpoint (Fig. 2b). With the knowledge gained from certain papers of accurately identified partial trisomy 21 that have been published in the past few years [Forster-Gibson et al., 2001; Rost et al., 2004; Kosaki et al., 2005; Kondo et al., 2006; Ronan et al., 2007], we narrow down the DSCR to a region between the proximal boundary of DS1 [Ronan et al., 2007] and the distal

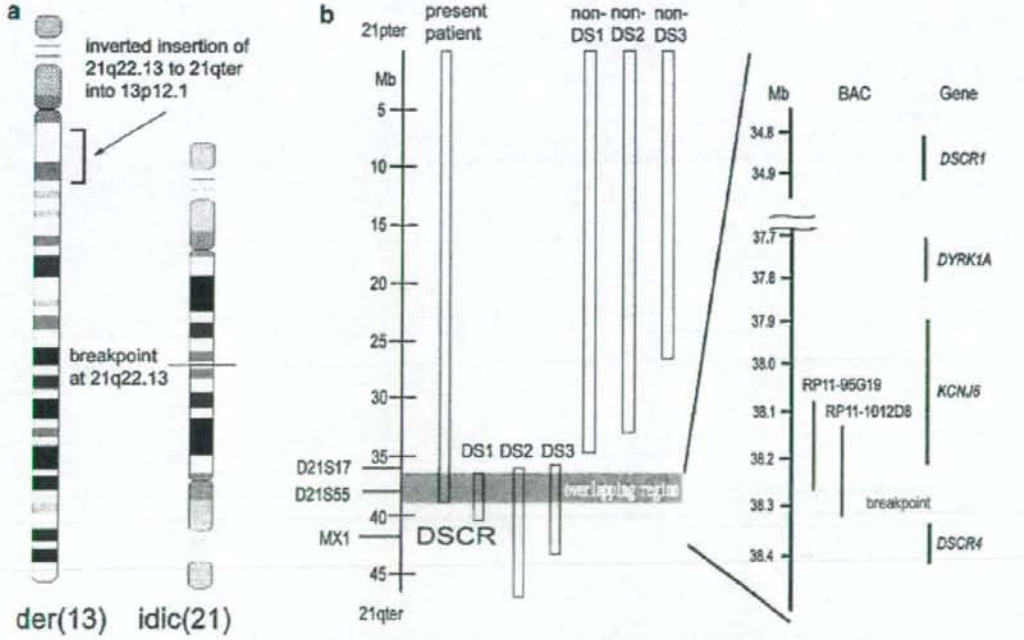

FIG. 2. **a**: Ideogram of der(13) and der(21) of the patient, showing trisomy for 21pter-q22.13 and disomy for 21q22.13-qter. **b**: Relationship between the DSCR and trisomic segments of the present DS patient and recently reported three non-DS cases; non-DS1 and DS2 [Kondo et al., 2006] and non-DS3 [Rost et al., 2004] and three other DS patients; DS1 [Ronan et al., 2007], DS2 [Forster-Gibson et al., 2001], and DS3 [Kosaki et al., 2005]. Enlargement of the overlapping region containing RP11-1012D8 with split FISH signals and its contiguous clone (RP11-95G19) without split signal. *KCNJ6* and *DSCR4* are the closest known genes flanking the breakpoint.

border of our patient, from RP11-957K9 located on 21q22.12 to RP11-1012D8 on 21q22.13, approximately 2.3 Mb in size (Fig. 2b) from the previous estimated 5.4 Mb DSCR at 21q22. [Delabar et al., 1993; Arron et al., 2006]. Since our patient manifested most of the main features of DS, we propose that the newly limited DSCR plays a role of the occurrence of DS in humans. A segment distal to the RP11-1012D8 may not attribute to the DS phenotype as far as our patient is concerned. Our data may support the studies by Arron et al. in mice. Because *DYRK1A* gene is included in the DSCR described here but *DSCR1* is not (Fig. 2b), key role of *DYRK1A* could be applied for human.

In conclusion, we have reported on a girl with DS who had a de novo 46,XX,psu idic(21)(q22.13) ins(13;21)(q12.1;q22.13q22.3) karyotype that might provide a potential clue to minimize the DSCR.

ACKNOWLEDGMENTS

Participation of the patient and her parents in this study is highly appreciated. We also thank Ms. Y. Noguchi, K. Miyazaki and A. Goto for their technical assistance.

REFERENCES

Antonarakis SE, Lyle R, Dermitzakis ET, Reymond A, Deutsch S. 2004. Chromosome 21 and Down syndrome: From genomics to pathophysiology. Nature Rev Genet 5:725–738.

Arron JR, Winslow MM, Polleri A, Chang CP, Wu H, Gao X, Neilson JR, Chen L, Heit JJ, Kim SK, Yamasaki N, Miyakawa T, Francke U, Graef IA, Crabtree GR. 2006. NFAT dysregulation by increased dosage of *DSCR1* and *DYRK1A* on chromosome 21. Nature 441:595–600.

Delabar JM, Theophile D, Rahmani Z, Chettouh Z, Blouin JL, Prieur M, Noel B, Sinet PM. 1993. Molecular mapping of twenty-four features of Down syndrome on chromosome 21. Eur J Hum Genet 1:114–124.

Forster-Gibson CJ, Davies J, MacKenzie JJ, Harrison K. 2001. Cryptic duplication of 21q in an individual with a clinical diagnosis of Down syndrome. Clin Genet 59:438–443.

Jackson JF, North ER III, Thomas JG. 1976. Clinical diagnosis of Down's syndrome. Clin Genet 9:483–487.

Kondo Y, Mizuno S, Ohara K, Nakamura T, Yamada K, Yamamori S, Hayakawa C, Ishii T, Yamada Y, Wakamatsu N. 2006. Two cases of partial trisomy 21(pter-q22.1) without the major features of Down syndrome. Am J Med Genet Part A 140A: 227–232.

Kosaki R, Kosaki K, Matsushima K, Mitsui N, Matsumoto N, Ohashi H. 2005. Refining chromosomal region critical for Down syndrome-related heart defects with a case of cryptic 21q22.2 duplication. Congenital Anomalies 45:62–64.

Maraschio P, Zuffardi O, Lo Curto F. 1980. Cd bands and centromeric function in dicentric chromosomes. Hum Genet 54:265–267.

Olson LE, Richtsmeier JT, Leszl J, Reeves RH. 2004. A chromosome 21 critical region does not cause specific Down syndrome phenotypes. Science 306:687–690.

Olson LE, Roper RJ, Sengstaken CL, Peterson EA, Aquino V, Galdzicki Z, Siarey R, Pletnikov M, Moran TH, Reeves RH. 2007. Trisomy for the Down syndrome critical region is necessary but not sufficient for brain phenotypes of trisomic mice. Hum Mol Genet 16:774–782.

Ronan A, Fagan K, Christie L, Conroy J, Nowak N, Turner G. 2007. Familial 4.3Mb duplication of 21q22 sheds new light on the Down syndrome critical region. J Med Genet 44:448–451.

Rost I, Fiegler H, Fauth C, Carr P, Bettecken T, Kraus J, Meyer C, Enders A, Wirtz A, Meitinger T, Carter NP, Speicher MR. 2004. Tetrasomy 21pter-q21.2 in a male infant without typical Down's syndrome dysmorphic features but moderate mental retardation. J Med Genet 41:e26.

Sato D, Shimokawa O, Harada N, Olsen OE, Hou JW, Muhlbauer W, Blinkenberg E, Okamoto N, Kinoshita A, Matsumoto N, Kondo S, Kishino T, Miwa N, Ariga T, Niikawa N, Yoshiura K. 2007. Congenital arhinia: Molecular-genetic analysis of five patients. Am J Med Genet Part A 143A:546–552.

CELL BIOCHEMISTRY AND FUNCTION
Cell Biochem Funct 2008; **26**: 146–150.
Published online 17 April 2007 in Wiley InterScience
(www.interscience.wiley.com) **DOI**: 10.1002/cbf.1413

Decreased serum dependence in the growth of NIH3T3 cells from the overexpression of human nuclear receptor-binding SET-domain-containing protein 1 (*NSD1*) or fission yeast su(var)3-9, enhancer-of-zeste, trithorax 2 (*SET2*)

Toshiko Yamada-Okabe [1,2*] and Naomichi Matsumoto [1]

[1] *Department of Human Genetics, Yokohama City University Graduate School of Medicine, Japan*
[2] *Department of Food Science, Faculty of Arts and Sciences, Sagami Women's University, Japan*

Nuclear receptor-binding SET-domain-containing protein 1 (*NSD1*), a culprit gene for Sotos syndrome, contains a su(var)3-9, enhancer-of-zeste, trithorax (SET) domain that is responsible for histone methyltransferase activity and other domains such as plant homeodomain (PHD) and proline-tryptophan-tryptophan-proline (PWWP) involved in protein–protein interactions in the C-terminal half of NSD1. To elucidate the function of NSD1 on cell growth, we overexpressed NSD1 in NIH3T3 cells. Cells overexpressing NSD1 grew in the presence of 2% serum, whereas vector transfected cells did not. Overexpression of the C-terminal half of NSD1 but not the N-terminal half of NSD1 also produced cell growth under low serum concentration. Furthermore, overexpression in NIH3T3 of *Schizosaccharomyces pombe* SET2 which has a SET domain but not PHD or PWWP domains conferred the reduced serum dependence. Thus, the SET domain of NSD1 is involved in cell growth by modulating serum dependence. Copyright © 2007 John Wiley & Sons, Ltd.

KEY WORDS — SET domain; histone H3K36; NSD1; SET2; serum

INTRODUCTION

Nuclear receptor-binding SET domain protein 1 (*NSD1*) is the gene responsible for Sotos syndrome[1] which is characterized by rapid growth in childhood, distinctive craniofacial features including macrocephaly, and mental retardation. NSD1 protein contains a su(var)3-9, enhancer-of-zeste, trithorax (SET) domain and other functional domains including plant homeodomain (PHD) and proline-tryptophan-tryptophan-proline (PWWP) domains, both of which are involved in protein–protein interaction.[2] Most enzymes with histone methyltransferase activity contain a SET domain, and therefore, it has been considered that NSD1 also has histone methyltransferase activity. In fact, the recombinant protein-containing SET domain of NSD1 was demonstrated to have the ability to methylate lysine 36 of histone H3 and lysine 20 of histone H4.[3] Embryos of NSD1-deficient mice showed apoptosis at E7.5–E8.0, indicating that NSD1 protein is essential for gastrulation and development in mice. However, the physiological role of NSD1 remains to be elucidated.

In order to gain more insight into the physiological role of NSD1, we constitutively expressed it in NIH3T3 cells. We found that NIH3T3 cells expressing NSD1 were able to proliferate even under the condition of a low serum concentration, and that the C-terminal region containing the SET domain of NSD1 was essential for the decreased serum dependence. Similar results were obtained from the expression of *Schizosaccharomyces pombe* (*S. pombe*) SET2 which contains a SET domain but not a PWWP or PHD domain. The results indicate that the SET domain of NSD1 positively regulates cell growth.

* Correspondence to: T. Yamada-Okabe, Department of Food Science, Faculty of Arts and Sciences, Sagami Women's University, 2-1-1 Bunkyo, Sagamihara, Kanagawa 228-8533, Japan. Tel/Fax: +81-42-742-1945. E-mail: t-okabe@star.sagami-wu.ac.jp

Received 3 January 2007
Revised 14 February 2007
Accepted 22 February 2007

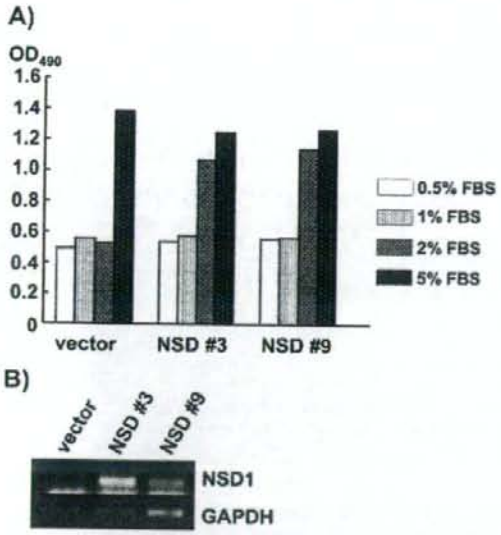

Figure 1. Reduced serum dependence from the constitutive expression of *NSD1* in NIH3T3 cells. (A) One thousand cells per well were plated on 96-well microplates and were cultured in the absence or presence of 0.5, 1, or 2% FBS. After 14 days, 20 μL of CellTiter 96 AQ_{ueous} One Solution Reagent was added to the cells, and the cells were further incubated for 3 h. Absorbance at 490 nm, which correlates with the viable cell number, is shown. The two independent clones which overexpressed NSD1 in NIH3T3 cells were designated NSD#3 and NSD#9. (B) Expression of *NSD1* was confirmed by RT-PCR. The obtained PCR products were analyzed by agarose gel electrophoresis

MATERIALS AND METHODS

Isolation of S. pombe SET2-related gene

Genomic DNA of *S. pombe* was prepared from the L972 strain as described.[4] *S. pombe* cells were treated with zymolyase to disrupt the cell wall, and the resulting spheroplasts were lysed by 1% SDS. After digesting RNA with 0.1 mg ml^{-1} RNaseA at 37 °C for 1 h, genomic DNAs were precipitated by ethanol. The *S. pombe* SET2 gene was cloned by PCR using a set of primers, 5′-GAGCCCGGGATGCAGACGGCATCATCTCT-3′ and 5′-GAGCCCGGGTTAAGCAGCTTTTTTCGGGG-3′. Human NSD1 cDNA and *S. pombe* SET2 were cloned at the *Sca*I site of pCruz-His (Santa Cruz Biotechnology, Inc., CA) and the *Eco*RV site of pCruz-His (Santa Cruz), respectively, to drive human NSD1 cDNA and *S. pombe* SET2 transcription from the CMV promoter. NIH3T3 cells were transfected with pCruz-His (Santa Cruz) or pCMV-Tag4 (Stratagene, CA, USA) carrying the human NSD1 cDNA or *S. pombe* SET2 by Lipofectamine™ (Invitrogen, CA, USA). After selection with 0.5–1 mg ml^{-1} G418 for 2 weeks, G418-resistant clones which expressed NSD1 or SET2 were selected and used for the experiments.

GenBank accession numbers for human NSD1 and *S. pombe* SET2 are AF395588 and NM001020411, respectively.

Cell proliferation assay

Cells (1.5×10^3) of NIH3T3 expressing or not expressing human NSD1 or *S. pombe* SET2 were cultured in 100 μL of medium in the absence or presence of 0.5, 1, 2, or 5% of fetal bovine serum at 37 °C for at least 7 days. The vector-transfected NIH3T3 cells were used as the control. At the end of the culture, 20 μL of CellTiter 96 AQ_{ueous} One Solution Reagent (Promega, WI, USA) containing 5-(3-carboxymethoxyphenyl)-2-(4, 5-dimenthylthiazoly)-3-(4-sulfophenyl) tetrazolium salt (MTS) was added to the medium, and the cells were incubated at 37 °C for 1–4 h. Absorbance at 490 nm, which represents the amount of formazan product and thereby viable cell number, was measured using a microplate reader (BioRad, CA, USA).

RT-PCR

One microgram of total RNA was used for single-stranded cDNA synthesis. After reverse-transcriptase reaction, the cDNA was amplified by 25 cycles of consecutive incubations at 94 °C for 30 s, 60 °C for 30 s, and 72 °C for 60 s with primers for the indicated cDNA and RNA LA PCR kit (AMV) Ver 1.1 (Takara, Shiga, Japan).

The primer sequences for PCR were 5′-CCCAGGATGGATCAGACCTGTGAAC-3′, 5′-AGCAGACCCATTTAAATACTCTAC-3′, 5′-TATTTGTGGACTCACCAAGCCCGAGTCTTC-3′, and 5′-TGCAGTGAAGATCTGTACCCTGCC-3′ for *NSD1*, and 5′-GAGCCCGGGATGCAGACGGCATCATCTCT-3′ and 5′-TTTCTTTTCGGTTAAGAAAACATCCACCTT-3′ for *S. pombe SET2*.

RESULTS AND CONCLUSIONS

Effects of overexpression of NSD1 on cell growth

Sotos syndrome, accompanied by rapid growth in childhood, is caused by haploinsufficiency of *NSD1*.[1] Therefore, we asked whether *NSD1* is involved in cell growth under certain circumstances. Therefore, *NSD1* was expressed constitutively in NIH3T3 under the CMV promoter (Figure 1B). Constitutive expression

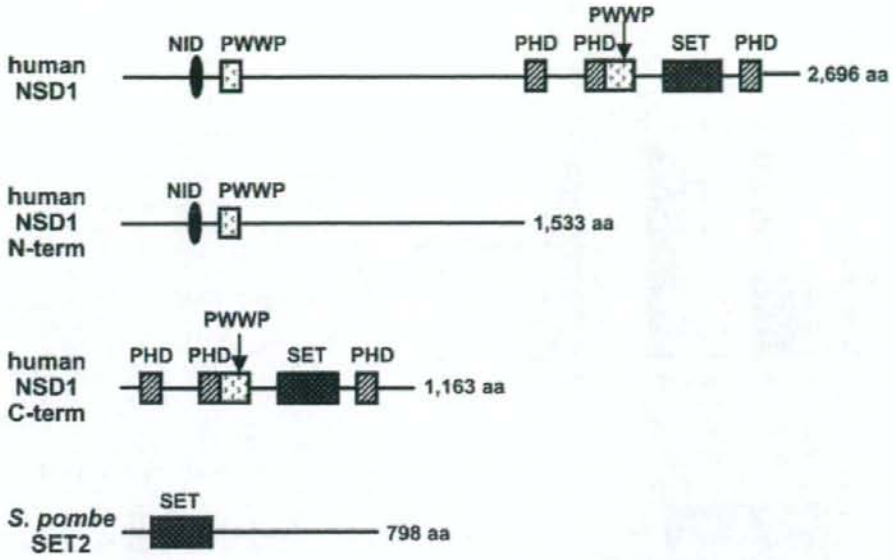

Figure 2. Domain structures of total human NSD1, N- and C-terminal halves of NSD1, and *S. pombe* SET2

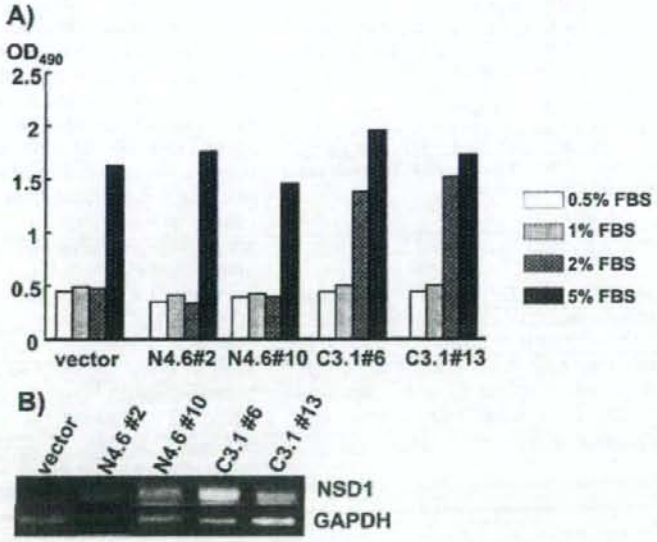

Figure 3. Reduced serum dependence from the constitutive expression of the C-terminal half of NSD1 in NIH3T3 cells. (A) One thousand cells per well were plated on 96-well microplates and were cultured in the absence or presence of 0.5, 1, or 2% FBS. After 14 days, 20 μL of CellTiter 96 AQ_{ueous} One Solution Reagent was added to the cells, and the cells were further incubated for 3 h. Absorbance at 490 nm, which correlates with the viable cell number, is shown. The independent clones which overexpressed in the N-terminal half and in the C-terminal half of NSD1 in NIH3T3 cells were designated N4.6#2 and N4.6#10 and C3.1#6 and C3.1#10, respectively. (B) Expression of *NSD1* mRNA fragments in the N-terminal half or the C-terminal half of *NSD1* was confirmed by RT-PCR. The obtained PCR products were analyzed by agarose gel electrophoresis

DOI: 10.1002/cbf

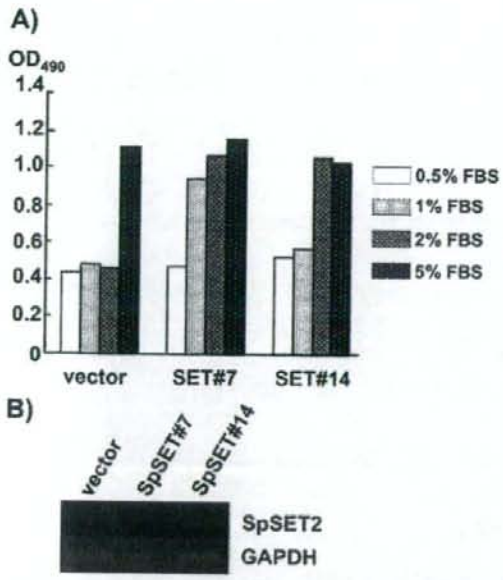

Figure 4. Reduced serum dependence from the constitutive expression of *S. pombe* SET2 in NIH3T3 cells. (A) One thousand cells per well were plated on 96-well microplates and were cultured in the absence or presence of 0.5, 1, or 2% FBS. After 14 days, 20 μL of CellTiter 96 AQ_{ueous} One Solution Reagent was added to the cells, and the cells were further incubated for 3 h. Absorbance at 490 nm, which correlates with the viable cell number, is shown. The two independent clones which overexpressed SET2 in NIH3T3 cells were designated SET#7 and SET#14. (B) Expression of the *SET2* mRNA was confirmed by RT-PCR. The obtained PCR products were analyzed by agarose gel electrophoresis

of NSD1 did not affect the growth of the cells when the cells were cultured with 10% FBS. However, cells expressing NSD1 were able to proliferate even in 2% serum, whereas the vector-transfected cells did not grow in such a low concentration of serum, as indicated by the results from two independent clones, #3 and #9, compared to the control (Figure 1A).

SET domain was necessary for decreased serum dependence

NSD1 contains a nuclear receptor interacting domain (NID) in the N-terminal half, 2 PWWP domains (1 in each half), 3 PHD domains in the C-terminal half, and a SET domain in the C-terminal half (Figure 2). Translocation of the NSD1 gene to the NUP98 locus, t(5;11)(q35;p15.5), causes childhood acute myeloid leukemia,[5] and the SET domain has been considered to be involved in the cell cycle. We examined whether the C-terminal half of NSD1 affects cell proliferation. The results show that decreased serum dependence was reproduced by the constitutive expression of the C-terminal half of NSD1, as indicated by a comparison of independent clones C3.1#6 and C3.1#13 with the control, but not by the N-terminal half, as indicated by a comparison of independent clones N4.6#2 and N4.6#10 with the control (Figure 3A).

S. pombe SET2 has a SET domain but no other domains present in NSD1 (Figure 2). To further confirm that the decreased serum dependence is largely attributable to the function of the SET domain, we constitutively expressed the *S. pombe* SET2 gene in NIH3T3 cells and found that the cells expressing *S. pombe* SET2 also grew in 2% serum, indicated by the comparison of clones #7 and #14 with the control (Figure 4A).

The SET domain of NSD1 methylates lysine 36 of histone H3 and lysine 20 of histone H4 *in vitro*,[3] whereas the *S. pombe* Set2 protein methylates only lysine 36 of histone H3.[6] Because the constitutive expression of *S. pombe* SET2 decreased the serum dependence of NIH3T3, the ability to methylate lysine 36 of histone H3 seems to be important for a decrease of serum dependence in cell growth. Yeast *Saccharomyces cerevisiae* and *S. pombe* Set2 proteins have been reported to be associated with the hyperphosphorylated form of RNA polymerase II,[6–9] and thus methylation of lysine 36 of histone H3 may be related to transcriptional activation. It has been reported that histone H3 modification with phosphorylation and acetylation correlates with the cell cycle.[10] Furthermore, methylation of lysine 36 in histone H3 is necessary for normal development in *Neurospora crassa*[11] and prevention of early flowering in *Arabidopsis thaliana*.[12] On the other hand, methylation of lysine 20 of histone H4 has been found in heterochromatin,[13] which implies that methylation of lysine 20 of histone H4 may cause transcriptional repression. It may be of interest to clarify whether methylation activity of lysine 20 of histone H4 is also necessary for the stimulation of growth in low concentrations of serum.

ACKNOWLEDGEMENTS

This work was supported in part by a grant-in-aid from the Ministry of Education, Culture, Sports, Science and Technology of Japan to NM.

REFERENCES

1. Kurotaki N, Imaizumi K, Harada N, *et al.* Haploinsufficiency of NSD1 causes Sotos syndrome. *Nat Genet* 2002; **30**: 365–366.
2. Kurotaki N, Harada N, Yoshiura K, Sugano S, Niikawa N, Matsumoto N. Molecular characterization of NSD1, a human homologue of the mouse Nsd1 gene. *Gene* 2001; **279**: 197–204.
3. Rayasam GV, Wendling O, Angrand P-O, *et al.* NSD1 is essential for early post-implantation development and has a catalytically active SET domain. *EMBO J* 2003; **22**: 3153–3163.
4. Hoffman SC. 1997; Preparation of yeast DNA. In *Current Protocols in Molecular Biology*, Ausubel FM, Brent R, Kingston RE, Moore DD, Seidman JG, Struhl K (eds). John Wiley and Sons: 13.11.1–13.11.4.
5. Brown J, Jawad M, Twigg SRF, *et al.* Acryptic t(5;11)(q35;p15.5) in 2 children with acute myeloid leukemia with apparently normal karyotypes, identified by a multiplex fluorescence *in situ* hybridization telomere assay. *Blood* 2002; **99**: 2526–2531.
6. Morris SA, Shibata Y, Noma K, *et al.* Histone H3 K36 methylation is associated with transcription elongation in *Schizosaccharomyces pombe*. *Eukaryot Cell* 2005; **4**: 1446–1454.
7. Strahl BD, Grant PA, Briggs SD, *et al.* Set2 is a nucleosomal histone H3-selective methyltransferase that mediated transcriptional repression. *Mol Cell Biol* 2002; **22**: 1298–1306.
8. Schaft D, Roguev A, Kotovic KM, *et al.* The histone 3 lysine 36 methyltransferase, SET2, is involved in transcriptional elongation. *Nucl Acids Res* 2003; **31**: 2475–2482.
9. Kizer KO, Phatnani HP, Shibata Y, Hall H, Greenleaf AL, Strahl BD. A novel domain in set2 mediates RNA polymerase II interaction and couples histone H3 K36 methylation with transcript elongation. *Mol Cell Biol* 2005; **25**: 3305–3316.
10. McManus KJ, Hendzel MJ. The relationship between histone H3 phosphorylation and acetylation throughout the mammalian cell cycle. *Biochem Cell Biol* 2006; **84**: 640–657.
11. Adhvaryu KK, Morris SA, Strahl BD, Selker EU. Methylation of histone H3 lysine 36 is required for normal development in *Neurospora crassa*. *Eukaryot Cell* 2005; **4**: 1455–1464.
12. Zhao Z, Yu Y, Meyer D, Wu C, Shen W-H. Prevention of early flowering by expression of FLOWERING LOCUS C requires methylation of histone H3 K36. *Nat Cell Biol* 2005; **7**: 1256–1260.
13. Shotta G, Lachner M, Marma K, *et al.* A Silencing pathway to induce H3-K9 and H4-K20 trimethylation at constitutive heterochromatin. *Genes Dev* 2004; **18**: 1251–1262.

Cell Biochem Funct 2008; **26**: 146–150.
DOI: 10.1002/cbf

American Journal of Medical Genetics Part A 146A:1241–1247 (2008)

Two New Cases of Pure 1q Terminal Deletion Presenting With Brain Malformations

Yoko Hiraki,[1]* Nobuhiko Okamoto,[2] Tomoko Ida,[3] Yusei Nakata,[4] Masahiro Kamada,[5] Yonehiro Kanemura,[6] Mami Yamasaki,[6] Hiroko Fujita,[7] Gen Nishimura,[8] Mitsuhiro Kato,[9] Naoki Harada,[3,10] and Naomichi Matsumoto[10,11]

[1]Hiroshima Municipal Center for Child Health and Development, Hiroshima, Japan
[2]Osaka Medical Center and Research Institute for Maternal and Child Health, Osaka, Japan
[3]Department of Molecular Cytogenetics, Kyushu Medical Science, Inc., Nagasaki, Japan
[4]Medical Center for Premature and Neonatal Infants, Hiroshima City Hospital, Hiroshima, Japan
[5]Division of Pediatrics, Hiroshima City Hospital, Hiroshima, Japan
[6]Institute for Clinical Research and Department of Neurosurgery, Osaka National Hospital, Osaka, Japan
[7]Research Department, Mitsubishi Kagaku Bio-Clinical Laboratories, Tokyo, Japan
[8]Division of Radiology, Tokyo Metropolitan Kiyose Children's Hospital, Kiyose, Japan
[9]Department of Pediatrics, Yamagata University School of Medicine, Yamagata, Japan
[10]Solution-Oriented Research for Science and Technology, Japan Science and Technology Agency, Tokyo, Japan
[11]Department of Human Genetics, Yokohama City University Graduate School of Medicine, Yokohama, Japan

Received 25 July 2007; Accepted 15 December 2007

We describe two new cases of pure 1q terminal deletions. BAC FISH analysis precisely defined the size of deletions. The first is a girl with 10.3-Mb deletion showed typical features of 1q43 deletion as well as a simplified gyral pattern, which was rarely found in 1q43 deletion. The other boy also presented with most of 1q43 deletion features but several atypical symptoms were noted including hydrocephalus, adducted thumbs, and flexion restriction of proximal interphalangeal joints in left hand. A concomitant novel missense mutation in *L1CAM* was identified in addition to 11.5-Mb deletion. Reviewing all the cases of pure 1q terminal deletion in the literature suggests that it is a clinically recognizable syndrome. © 2008 Wiley-Liss, Inc.

Key words: 1q terminal deletion; brain malformation; X-linked hydrocephalus; *L1CAM* mutation

How to cite this article: Hiraki Y, Okamoto N, Ida T, Nakata Y, Kamada M, Kanemura Y, Yamasaki M, Fujita H, Nishimura G, Kato M, Harada N, Matsumoto N. 2008. Two new cases of pure 1q terminal deletion presenting with brain malformations. Am J Med Genet Part A 146A:1241–1247.

INTRODUCTION

Since the first report of Mankinen et al. [1976], more than 50 deletions at 1q42-qter and uninvolved with other chromosomal abnormalities have been documented [Gentile et al., 2003; van Bever et al., 2005; Boland et al., 2007; Hill et al., 2007; Merritt et al., 2007]. These deletions may result in a recognizable phenotype including characteristic facial appearance, microcephaly, psychomotor retardation, and variable other anomalies [van Bever et al., 2005]. Most deletions were only cytogenetically examined, but detailed molecular mapping information is available in 14 cases [Gentile et al., 2003; van Bever et al., 2005; Kanemoto et al., 2006; Boland et al., 2007; Hill et al., 2007; Merritt et al., 2007; Poot et al., 2007].

Here we report on two new cases of pure 1q43-qter deletion with brain abnormalities, a simplified gyral pattern previously reported in two cases [Hill et al., 2007] and hydrocephalus. Deletions were precisely mapped by FISH analysis. Clinical features of pure 1q distal deletion from all the reported patients are summarized. Finally the hydrocephalus, which was

Grant sponsor: Ministry of Health, Labour and Welfare, Japan; Grant sponsor: JST.

*Correspondence to: Yoko Hiraki, M.D., Hiroshima Municipal Center for Child Health and Development, Hikarimachi 2-15-55, Higashi-Ku, Hiroshima 732-0052, Japan.
E-mail: hy-772v@enjoy.ne.jp
**Correspondence to: Naomichi Matsumoto, M.D., Ph.D., Department of Human Genetics, Yokohama City University Graduate School of Medicine, Fukuura 3-9, Kanazawa-ku, Yokohama 236-0004, Japan.
E-mail: naomat@yokohama-cu.ac.jp

DOI 10.1002/ajmg.a.32275

rare in 1q terminal deletion, turned out to be caused by a concomitant *L1CAM* mutation.

METHODS AND RESULTS

Subjects

Patient 1. The 5-year-old girl is the second product of an unrelated 31-year-old mother and 32-year-old father. She was born by cesarean at 38 weeks of gestation due to intrauterine growth retardation. Her birth weight was 2,190 g (−2.3 SD), length 40 cm (−4.6 SD), and OFC 30 cm (−2.1 SD). Multiple malformations included incomplete cleft palate, hemivertebra, talipes valgus, and tetralogy of Fallot (TOF) which was surgically repaired at her age of 1 year. At 15 months, she was referred to us for evaluation of her developmental delay. She had microcephaly (−4.4 SD), prominent metopic suture, sparse and fine hair, round face, thin and bow-shaped eyebrows, strabismus, upslanting palpebral fissures, periorbital fullness, hypertelorism, epicanthus, flat nasal bridge, short and broad nose, hypoplastic nares, smooth and long philtrum, thin vermilion borders, well formed "cupid's" bow, mouth with downturned corners, tucked in lower lip, micro/retrognathia, incomplete cleft palate, prominent antihelices, ear lobe clefts, left retroauricular fold, and short neck (Fig. 1A and Table I). Additionally, she had abnormal hands and feet consisting of small, edematous dorsum of hands and feet, tapering fingers, bilateral singular palmar creases, bilateral vertical tali, proximally placed 2nd toes, and scoliosis and bilateral accessory nipples were noticed. She was diagnosed as an autistic disorder, based on the DSM-IV. Autonomic dysfunctions were observed, such as gastric esophageal reflux (GER), deglutition abnormalities, abnormal sweating, flushing spells, peripheral coldness, and apneic spell. Her dysphagia with GER was treated during 1–3 years. At 2 years, her weight was 7,700 g (−3.0 SD), length 71.2 cm (−4.0 SD), and OFC 39.5 cm (−4.9 SD). Complex partial seizure requiring anticonvulsant treatment started at her 2 years, was deteriorated by influenza encephalopathy, leading to severe developmental delay at 5 years (DQ = 9). At age of 5 years, her weight was 11.8 kg (−2.4 SD), length 89.5 cm (−3.9 SD), and OFC 42.0 cm (−4.6 SD). She could sit alone and creep, but could not recognize her parents. Uncontrollable seizures and autonomic dysfunction persisted. She also had hypoplastic labia majora and minora. Stiff barrel-shaped thorax was also recognized. Brain magnetic resonance imaging (MRI) revealed microcephaly with a simplified gyral pattern, thin corpus callosum, and reduced white-matter volume (Fig. 1A). Echocardiography confirmed no other abnormalities. 1q distal deletion was suspected as she presented with growth and psychomotor retardation, typical craniofacial features, abnormal hands and feet, and other anomalies.

Patient 2. He was 5 years old and the first child of an unrelated 39-year-old mother and 48-year-old father. The mother had one spontaneous abortion at 7 weeks of gestation. In pregnancy, IUGR, large ventricles of fetal brain, and hydramnios were noted at the third trimester, and fetal karyotype was normal after fetal blood sampling. He was born by cesarean at 36 weeks. His birth weight was 1,242 g (−3.9 SD), length 39 cm (−3.1 SD), and OFC 27.6 cm (−2.9 SD).

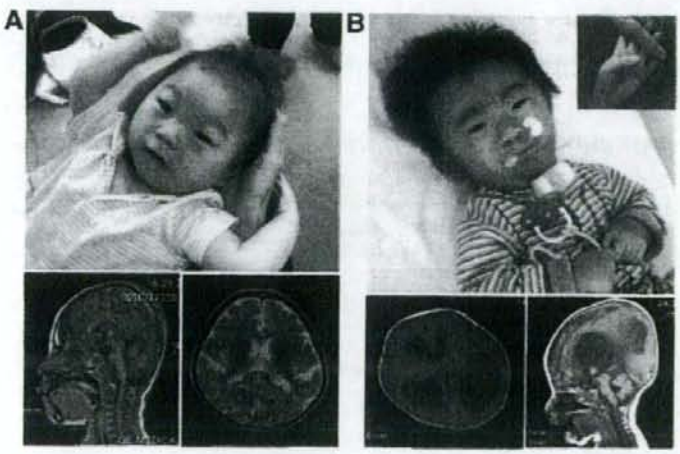

FIG. 1. A: Patient 1. Face at 19 months (upper), and MRI images at 5 years (lower left, sagital section; lower right, horizontal). Typical facial appearance of 1q distal deletion is seen. A simplified gyral pattern and thin corpus callosum were noted. B: Patient 2. Face at 19 months (upper) along with left hand, and MRI at 4 years (lower left, horizontal section; lower right, sagittal). Midface hypoplasia, bushy hair, and synophrys were recognized, which is rarely seen. Adducted thumb was demonstrated. MRI shows large massa intermedia and marked dilation of the lateral ventricles. Thin corpus callosum, stenosis of the Sylvius aqueduct, and mild pontocerebellar atrophy are observed.

TABLE I. Clinical Findings of Pure Type of Del(1q) Syndrome

Clinical features	Previously reported patients					Our patients	
	Pure type of 1q deletion (n = 53) M/F=20:33	1q42deletion (n = 22) M/F = 9:13	1q43deletion (n = 17) M/F = 3:14	1q44deletion (n = 6) M/F = 3:3	Interstitial deletion of 1q42–44 (n = 8) M/F = 5:3	Case 1	Case 2
General							
Growth retardation	37/42[a]	14/16	14/14	5/5	4/7	+	+
Psychomotor retardation	48/50	20/20	17/17	6/6	5/7	+	+
CNS anomalies	35/39	10/13	14/15	5/5	6/6	+	+
Agenesis/thin corpus callosum	26/28	6/8	11/11	4/4	5/5	+	+
Hydrocephalus	2/2	1/1	1/1	0/0	0/0	−	+
Communicating type	1/2	1/1	0/1	0/0	0/0	−	−
Non-communicating type	1/2	0/1	1/1	0/0	0/0	−	+
Hypotonia	25/28	13/15	8/8	3/4	1/1	+	+
Seizures	33/39	11/15	16/16	4/6	2/2	+	+
Autonomic dysfunction	18/18	9/9	6/6	3/3	0/0	+	+
Dysphagia/feeding difficulties	12/12	6/6	5/5	1/1	0/0	+	+
Craniofacial							
Microcephaly	41/47	18/20	15/17	5/6	3/4	+	−
Prominent metopic suture/trigonocephaly	9/14	5/7	2/4	2/3	0/0	+	−
Sparse, fine hair	10/12	6/7	2/2	1/2	1/1	+	−
Round face	16/16	10/10	2/2	2/2	2/2	+	−
Upslanting palpebral fissures	23/27	12/15	7/7	3/4	1/1	+	+
Epicanthic folds	32/34	18/19	11/12	2/2	1/1	+	−
Impression of hypertelorism	14/17	8/9	4/5	2/2	0/1	+	+
Vision, eye anomaly	18/20	11/11	4/5	2/2	1/2	+	+
Strabismus	14/20	9/13	2/3	2/3	1/2	+	+
Short, broad nose/flat nasal bridge	37/37	19/19	12/12	5/5	1/1	+	+
Smooth, long philtrum	14/17	9/11	2/3	2/2	1/1	+	+
Thin vermillion borders	20/21	11/12	6/6	3/3	0/0	+	+
Well formed "cupid's" bow	9/10	6/7	2/2	1/1	0/0	+	−
Downturned corners of the mouth	29/32	15/17	11/11	2/3	1/1	+	+
Micro/retrognathia	28/35	16/19	7/10	2/3	3/3	+	+
Abnormal palate	20/25	12/14	4/5	1/3	3/3	+	+
Low set/dysplastic ears	30/38	14/19	7/7	5/5	4/7	+	+
Short/webbed neck	29/33	15/16	10/11	3/4	1/2	+	+
Extremities							
Abnormal hands	19/33	12/15	4/11	2/4	1/3	+	+
Clinodactyly of the 5th fingers	7/14	5/9	2/4	0/0	0/1	−	−
Hypoplastic fingernails	4/13	3/9	0/2	1/1	0/1	−	−
Small hands	4/11	3/7	0/2	0/0	1/2	+	+
Tapering fingers	4/11	1/5	1/3	2/2	0/1	+	−
Shortened thumbs	3/10	3/7	0/2	0/0	0/1	−	−
Syndactyly	3/10	1/5	2/4	0/0	0/1	−	−
Polydactyly	2/9	1/5	1/3	0/0	0/1	−	−
Adducted thumbs	0/0	0/0	0/0	0/0	0/0	−	+
Flexion restriction of PIP joints	0/0	0/0	0/0	0/0	0/0	−	+
Abnormal feet	20/29	7/12	9/10	4/5	0/2	+	+
Urogenital							
Genital anomalies (male, female)	18/18, 5/11	9/9, 2/4	3/3, 3/6	2/2, 0/0	4/4, 0/1	+	+
Kidney/urine pathway anomalies	6/15	0/6	4/6	1/1	1/2	−	+

(*Continued*)

TABLE I. (*Continued*)

Clinical features	Previously reported patients					Our patients	
	Pure type of 1q deletion (n = 53) M/F = 20:33	1q42deletion (n = 22) M/F = 9:13	1q43deletion (n = 17) M/F = 3:14	1q44deletion (n = 6) M/F = 3:3	Interstitial deletion of 1q42–44 (n = 8) M/F = 5:3	Case 1	Case 2
Others							
Cardiac anomalies	18/37	9/18	4/12	3/3	2/4	+	+
Ventricular septal defect	13/13	7/7	4/4	1/1	1/1	−	+
Noncompaction of left ventricular myocardium	1/1	0/0	0/0	0/0	1/1	−	+
Skeletal anomalies	18/23	5/8	10/11	1/1	2/3	+	+
Dyssprondylism	8/12	3/6	4/5	0/0	1/1	+	+

[a]Number of patients having the feature/number of patients examined as to the feature. (These data are referred to Hum Genet 41:115–120, 1978; Jpn J Hum Genet 39:433–437, 1994; Am J Hum Genet 81:292–304, 2007; J Med Genet 38:175–178, 2001; Hum Genet 98:151–156, 1979; J Med Genet 25:211–212, 1988; Am J Med Genet A 117:251–254, 2003; Am J Med Genet 35:379–382, 1990; Am J Med Genet 80:396–398, 1998; Ann Genet 35:167–169, 1992; Am J Med Genet 22:685–694, 1985; Ann Genet 31:193–194, 1988; Hum Genet 42:333–337, 1978; Birth Defects Orig Artic Ser 12:131–136, 1976; Am J Med Genet 25:599–600, 1986; Am J Med Genet 28:371–376, 1987; Am J Med Genet A 143:599–603, 2007; An Esp Pediatr 11:729–732, 1978; Ann Genet 27:178–179, 1984; Am J Med Genet 40:488–492, 1991; Ann Genet 25:154–155, 1982; Ugeskr Laeger 143:2500–2502, 1981; Am J Med Genet A 138:68–69, 2005; Ann Genet 30:126–128, 1987; Am J Med Genet A 128:352–363, 2004; Am J Med Genet 98:103–106, 2001; Eur J Pediatr 155:720, 1996; Ann Genet 28:177–180, 1985; Clin Genet 35:289–292, 1989; Ann Genet 26:161–164, 1983; Am J Med Genet A 135:91–95, 2005; Am J Med Genet 24:1–6, 1986; Pediatrics 77:786, 1986; Acta Paediatr Jpn 30:696–702, 1988; Clin Genet 19:544–545, 1981; Eur J Med Genet 49:247–253, 2006.)

Multiple malformations were recognized including hydrocephalus, ventricular septal defect (VSD), left hydronephrosis, and hypospadias. A shunt operation for ventriculomegaly was not performed. Developmental delay was noticed soon after birth. At age of 6 months, he received tracheostomy because of prolonged respiratory distress, as well as orchidopexy and bilateral inguinal herniotomy. VSD was repaired at 1 year and his development was then evaluated. He could not control his head with hypotonia. Severe psychomotor delay, growth retardation and serious dysphagia were recognized. Facial features included macro/brachycephaly, bushy hair, midface hypoplasia, thick and bow shaped eyebrows, upslanting palpebral fissures, periorbital fullness, hypertelorism, flat nasal bridge, short and broad nose, hypoplastic alae nasi, smooth and long philtrum, thin vermilion borders, downturned corners of the mouth, tucked in lower lip, micrognathia, high arched palate, low-set ears, prominent antihelices, involuted and sticked helices, webbed neck and posterior low hair line (Fig. 1B and Table I). Other multiple abnormalities included barrel-shaped thorax, widely spaced nipples, hypospadias, abnormally placed anus, abnormal hands and feet consisting of bilateral single transverse creases, small and edematous hands and feet, an adducted left thumb and severe restriction of PIP joints of a left hand and overlapping of the 1st toes over the 2nd toes (Fig. 1B). Abnormal eye movement, GER, butterfly vertebra of T4, and scoliosis were recognized. At age of 18 months, his weight was 6,380 g (−3.7 SD), length 68.5 cm (−3.5 SD), and OFC 46.5 cm (−0.9 SD). His DQ at $3^4/_{12}$ years was scored as 15. At age of 5 years, his weight was 13.6 kg (−1.6 SD), length 94.0 cm (−2.9 SD) and OFC 52.0 cm (+0.75 SD). He could take away towels covering his favorite toys, but he could not control his head with hypotonia, or recognize his parents. Tube feedings were required. Occasional burst of laughter and supraversion of his eyeballs were observed without any paroxysmal discharge. Delayed bone age (≤2 SD) were noticed. At age of $5^4/_{12}$ years, he had repeated bleeding from the orifice of tracheostomy. Embolotherapy of left subclavian artery collateral vessels was performed to prevent bleedings and cardiac ultrasonography revealed noncompaction of the left ventricular myocardium (NCLVM). Brain MRI revealed obstructive hydrocephalus associated with stenosis of aqueduct and marked dilation of lateral ventricles as well as large massa intermedia, thin corpus callosum, and mild pontocerebellar atrophy (Fig. 1B). Moderate left sensorineural hearing loss was noted. Left hydronephrosis with normal renal function was gradually ameliorated.

Genetic Analyses

G-banded chromosomal analysis of peripheral blood leukocytes indicated that both karyotypes of

Patients 1 and 2 were del(1)(q43) (Fig. 2 A,B). Fluorescence in situ hybridization (FISH) analysis using all chromosomal subtelomeric clones [Vysis ToTelVysion™ Multicolor FISH probe panel VYS-33-270000 (Abbott, Tokyo, Japan)] documented that both were a pure type of 1q terminal deletion as no other subtelomeric clones did show any abnormalities. Detailed FISH using BACs mapped to 1q42-1qter was performed as previously described [Shimokawa et al., 2005]. Deletions in Patients 1 and 2 were 10.3 Mb (from RP11-201D24 to 1q telomere) and 11.5 Mb (from RP11-1078D23 to telomere) in size, respectively (Fig. 2C). Parental chromosomes of both patients were normal. Since macro/brachycephaly, hydrocephalus and adducted left thumb in Patient 2, were not reported in 1q distal deletion and might be associated with L1-associated diseases, *L1CAM* was tested. Using genomic DNA from peripheral leukocytes as a template, all *L1CAM* exons were amplified by PCR, purified and subsequently sequenced using the BigDye Terminator Cycle Sequencing kit (Applied Biosystems, Foster City, CA). A novel missense mutation (c.92T → C: p.Val31Ala) in exon 3 was identified, and his mother was a heterozygous carrier (Fig. 3). Father was not tested. P.Val31 is evolutionally conserved through mammals and we sequenced more than 200 alleles and observed the same base pair change in another affected patient, but never in other patients or family members through the study of LI-associated diseases (data not shown). Thus we concluded that the nucleotide change was pathogenic.

DISCUSSION

Deletion from the 1q telomere is now proposed as a specific clinical syndrome [van Bever et al., 2005]. We have summarized clinical features of 53 cases of pure 1q distal deletions with reasonable clinical description (Table I). Among these, 22 patients were described as 1q42-qter deletion, 17 with 1q43-qter deletion, 6 with 1q44-qter deletion and 8 with interstitial deletion around 1q42-q44 [Mankinen et al., 1976; Gentile et al., 2003; van Bever et al., 2005; Kanemoto et al., 2006; Boland et al., 2007; Hill et al., 2007; Merritt et al., 2007]. We could successfully extract common clinical features of 1q distal deletions such as growth and psychomotor retardation, hypotonia, seizure, autonomic dysfunction, microcephaly, agenesis of corpus callosum possibly associated with *AKT3* haploinsufficiency [Boland et al., 2007], specific facial features, abnormal hands/

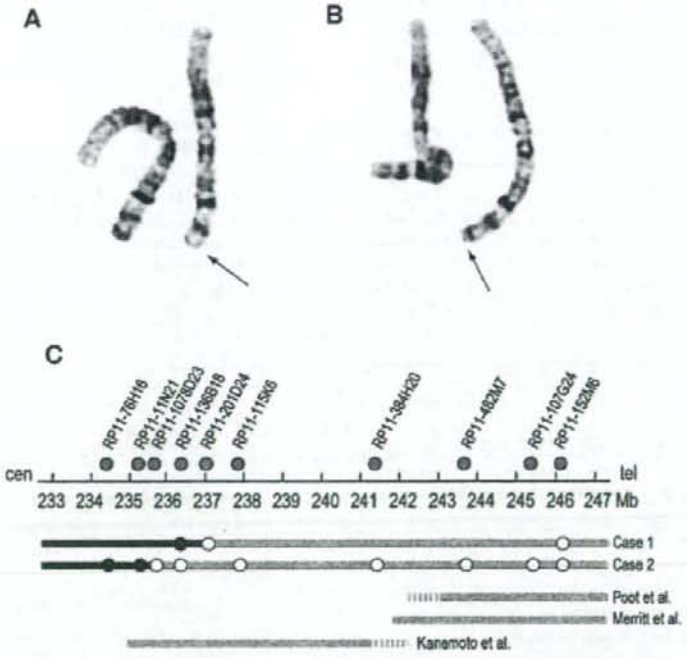

FIG. 2. Partial karyotype of Patients 1 (A) and 2 (B) and schematic presentation of 1q43-qter deletions (C). A,B: Arrow indicates deletion. C: Above the genomic scale, position of BAC clones was indicated as gray circle. Thick gray lines indicate deletion while black intact. White and black circles are BAC clones mapped to deleted and intact regions, respectively. Minimal critical regions for the 1q terminal deletion syndrome [Merritt et al., 2007; Poot et al., 2007] as well as an interstitial deletion associated with the noncompaction of left ventricular myocardium [Kanemoto et al., 2006] are depicted.

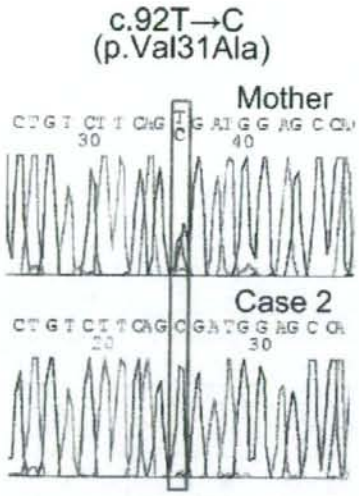

Homo sapiens L1CAM	EEYEGHHMMEPPVIT
Mus musculus XP_549364.2	DEYKGHHVLEPPVIT
Rattus norvesicus NP_059041.1	DEYKGHHVLEPPVIT
Canis familialis XP_549364.2	DEYEGYRVMEPPVIT
Equus caballus XP_001461834.1	HGHPGHHMMEPPVIT
Bos Taurus XP_594145.2	EEYEGHHMMEPPIIT

FIG. 3. A missense mutation, c.92T→C (p.Val31Ala) at exon 3 of *L1CAM* in Patient 2 (lower) and his mother (upper). Clustal W demonstrated that p.Val31 is evolutionally conserved through mammals (CLUSTALW ver. 1.83: http://clustalw.ddbj.nig.ac.jp/top-j.html). [Color figure can be viewed in the online issue, which is available at www.interscience.wiley.com.].

feet, and urogenital anomalies. Using this summary, we could propose that Patient 1 presented with a typical phenotype of 1q distal deletion. A simplified gyral pattern of brain was recently described in two cases [Hill et al., 2007], which may be due to abnormal neuronal and glial proliferation [Barkovich, 2005] and could be causative for uncontrollable seizures.

In Patient 2, several atypical conditions such as hydrocephalus, sensorineural hearing loss, left adducted thumb and restricted flexion of PIP joints were noticed in addition to many representative features of 1q distal deletion. Hydrocephalus associated with aqueductus stenosis, adducted left thumb, and mother's miscarriage history prompted us to test *L1CAM* for X-linked hydrocephalus (XLH). As expected, a novel missense mutation was identified. To our best knowledge, this is the first case of 1q distal deletion with accompanying XLH. The mutation was also recognized heterozygously in the mother. On the contrary, 1q distal deletion occurred as de novo. The *L1CAM* mutation (p.Val31Ala) in exon 3 is located at a signal peptide domain, which exists as an extracellular N-terminal region. P.Val31 is evolutionally conserved and the nucleotide change was recognized in another affected patient with an L1-associated disease. It belongs to class II mutations (amino acid substitutions in the extracellular part of L1 protein), raging from severe to mild phenotypes of L1-assosiated diseases [Yamasaki et al., 1997; Kanemura et al., 2006]. The NCLVM found in Patient 2 and another [Kanemoto et al., 2006] is intriguing. The overlapping 6.4-Mb region of the two deletions may harbor a gene(s) for the rare heart phenotype (Fig. 2C). Fetal blood karyotype by conventional chromosomal analysis was normal. When some brain malformations are recognized at ultrasound evaluation in prenatal periods, molecular techniques such as subtelomeric FISH/array CHG are encouraged in order to detect abnormal submicroscopic chromosomal changes.

In conclusion, two new cases of 1q43-qter deletions are described, who present with brain malformations: a simplified gyral pattern in Patient 1 and hydrocephalus with aqueductus stenosis in Patient 2. Each deletion was cytogenetically visible, precisely mapped by FISH, and was much larger than a 4.9–5.4-Mb minimal critical region (10.3 Mb and 11.5 Mb in size) (Fig. 2) [Merritt et al., 2007; Poot et al., 2007]. It may be challenging to delineate the phenotype/genotype correlation for pure 1q terminal deletion as most of deletions contain the minimal critical region for the syndrome. The simplified gyral pattern is reported as in the 3rd case. The hydrocephalus and other atypical features led to identification of a concomitant *L1CAM* mutation, being the first report in association with 1q distal deletion. Finally, the NCLVM associated with 1q terminal deletion found in this study is unique, while NCLUM has been observed in other chromosome conditions; this is the first report in 1q terminal deletion. This observation may be useful for narrowing down a disease locus.

ACKNOWLEDGMENTS

We are grateful to Dr. R. Kawamura and the staff of the rehabilitation institution 'Futaba En' for handicapped children, who have given habilitation and education to our patients. In addition, we thank Mr. Y. Unesaki, the physical therapist who provided beneficial information to us. This study was supported by Research Grant from the Ministry of Health, Labour and Welfare (N. M.) and SORST from JST (N.M.).

REFERENCES

Barkovich AJ. 2005. Pediatric neuroimaging. 4th edition. Philadelphia: Lippincott Williams & Wilkins. pp 329–332.

Boland E, Clayton-Smith J, Woo VG, McKee S, Manson FDC, Medne L, Zackai E, Swanson EA, Fitzpatrick D, Millen KJ, Sherr EH, Dobyns WB, Black GCM. 2007. Mapping of deletion and translocation breakpoints in 1q44 implicates the serine/